Check for updates

Moving while you're stuck: a macroscopic demonstration of an active system inspired by binding-mediated transport in biology†

Kanghyeon Koo,[a] Shankar Lalitha Sridhar,[bc] Noel Clark,[d] Franck Vernerey ⓘ *[b] and Loren Hough ⓘ *[cd]

Diffusive motion is typically constrained when particles bind to the medium through which they move. However, when binding is transient and the medium is made of flexible filaments, each association or dissociation event produces a stochastic force that can overcome the medium stickiness and enable motion. This mechanism is amply used by biological systems where the act of balancing binding and displacement robustly achieves key functionalities, including bacterial locomotion or selective active filtering in cells. Here we demonstrate the feasibility of making a dynamic system with macroscopic features, in which analogous binding-mediated motion can be actively driven, precisely tuned, and conveniently studied. We find an optimal binding affinity and number of binding sites for diffusive motion, and an inverse relationship between viscosity and diffusivity.

Active biological systems employ intricate and dynamic networks of flexible polymers to mediate various functionalities in real-time. Classic examples include the solid–fluid transition of the cell cytoskeleton in a matter of seconds,[1] the bacterial use of active pili fluctuations for locomotion,[2] or the selective transport of macromolecules through the nuclear pore complex.[3] For biopolymer networks like alginates, collagen or agarose, the continuous dissociation and association of cross-linking junctions that bind polymer chains can produce diverse mechanical responses.[4–6] Despite their stochastic nature and delicate energetics, these bio-networks produce emergent dynamic phenomena that are strikingly robust, evidence for the hand of evolution in system design, materials selection, and parameter tuning. Significant efforts have been directed toward using cellular biophysics and biochemical tools to understand and, more broadly emulate, modify, and apply such behavior in the lab.[7–9] This endeavor is hindered by (a) our inability to accurately control and tune independent chemical processes, and (b) challenges associated with introducing targeted and tunable activity in a non-biological system. Alternatively, active

granular materials and tunable mechanical metamaterials, by utilizing control afforded through larger-scale components and external driving, offer opportunities to widely explore novel mechanisms, visualize unexpected behavior, and build materials with unique functionalities.[10,11] The ability to selectively introduce activity has made active granular materials a major subfield of soft matter physics, and we propose that such an approach can be similarly powerful in this biophysical context.

Here, we present a prototypical design of a macroscopic dynamic system that can act as a medium for the transport of macroscopic objects, as inspired by the nuclear-pore complex. The system includes analogues to flexible filaments that can bind to a host *via* transient connections and are powered by active noise. With precision and control available due to its macroscopic nature, it effectively enables the exploration of the interplay between geometry, fluctuations, and binding to produce tunable viscosity and motion. Interestingly, while the fluctuation–dissipation theorem suggests that binding should slow down diffusion,[12–14] we find that in specific regimes, these events can enhance transport owing to the active nature of the system. Such counterintuitive emergent behavior is a hallmark of metamaterials, akin to phononic materials with negative mass[15] or auxetic structures with negative Poisson ratios.[16] In that light, our system can be seen as a prototypical subunit for building an active metamaterial inspired by biological dynamic networks.[17]

We concentrate on the physics of polymeric networks that utilize binding rather than collisions to control the diffusion of particles. A dynamic process of binding and unbinding combined with the structural reconfiguration of the polymer network

---

[a] *Civil, Environmental and Architectural Engineering, University of Colorado Boulder, Boulder, CO 80309, USA*

[b] *Mechanical Engineering, University of Colorado Boulder, Boulder, CO 80309, USA. E-mail: franck.vernerey@colorado.edu*

[c] *BioFrontiers Institute, University of Colorado, Boulder, USA*

[d] *Department of Physics, University of Colorado Boulder, Boulder, CO 80309, USA. E-mail: loren.hough@colorado.edu*

† Electronic supplementary information (ESI) available. See DOI: 10.1039/d0sm01808b

enables a form of actively driven facilitated diffusion of arbitrary particle sizes.[18,19] Some biopolymer networks act as filters, allowing the selective passage of specific molecules by tuning both particle concentration (*via* binding affinity) and particle mobility (*via* effective diffusion constant).[3,20] Theoretical studies describing the motion of particles through networks of polymeric binding sites have typically been developed for the nuclear pore complex (NPC), where transport factors bind transiently to long, flexible filaments called FG Nups.[18,21–23] In these systems the increase in net rate of transport through the network of particles that do bind is primarily driven by the motion of the particles while bound to the network, as motion while free is identical to that of particles that do not bind.[20] As a result, we are particularly interested in isolating the effects of polymer binding on the particle motion. The combination of binding site flexibility and rapid binding kinetics has two effects on particle motion. First, the polymeric binding motifs does, at least partially, constrain the motion of the bound particle,[19,24] in which case the residual motion of the bound particle can greatly increase the flux of binding particles.[20] In addition, binding is predicted to result in a stochastic driving force if the polymer binds in an extended conformation.[13,25,26] The interplay between constraint and driving is not well understood. Moreover, these effects all occur within a fluid context, with the fluid providing additional stochastic force that, in the absence of the polymers, would drive diffusive motion.

To simplify the problem and construct its corresponding experimental analogue, we first sought to determine whether we could separate the effects of the polymeric system and the surrounding fluid. Using an idealized diffusive plate model (Fig. 1a), we show that this is possible under relevant conditions, as described in more detail in related theoretical work.[27] These conditions restrict the analysis to systems (equilibrium or active) for which the fluctuation–dissipation theorem holds with an effective temperature (T_c for the chains), so that the effective friction coefficients are related to the diffusivities by $\zeta_c = k_B T_c / D_c$ (due to the chain attachments) and $\zeta_p = k_B T / D_p$ (of the plate due to the surrounding fluid), where k_B is the Boltzmann constant. We expect the diffusion constant to be:

$$D(N_a) = k_B \frac{\zeta_p T + \zeta_c T_c}{(\zeta_p + \zeta_c)^2}. \tag{1}$$

What remains is to determine ζ_c (or D_c) and T_c for the chains themselves.
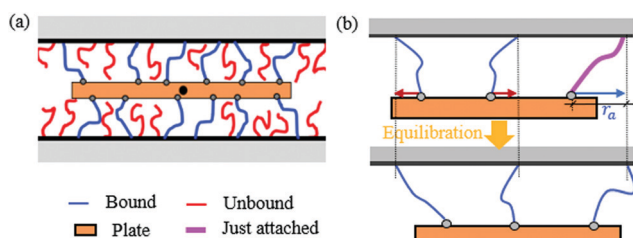

Fig. 1 (a) The idealization of the diffusive plate model with reversible binding and unbinding of polymer tethers. (b) The plate diffusion caused by the thermal fluctuation of the tethers during binding and unbinding events.

Having separated out the contribution of polymer binding from that of the surrounding media allowed us to focus on the question of the relative contributions of driving due to binding and unbinding events and restraint from the previously attached tethers. Our primary objective is thus to devise a tunable experimental system which allows us to easily change parameters that are relatively inaccessible in many biological systems. For instance, is it possible to create a material system whose transport properties and effective viscosity can be easily controlled by simply adjusting the supplied energy? An experimental system demonstrating binding driven motion and allowing easy tuning of relevant parameters would enable the rational design of a new generation of active metamaterials enabling particle transport and segregation based on geometry, size and properties, and be used as a material whose stiffness and viscosity can be varied in real time.

In order to experimentally determine the relative contributions of driving and inhibition due to binding to flexible tethers, we designed a macroscopic experimental system that incorporates polymer binding and restoring forces due to binding to extended chains. Our devised system consists of magnetic particles whose transient attachment to magnets on the surface of a cylinder drives the rotational diffusion of the cylinder (Fig. 2 and Fig. S1, ESI†). The cylindrical symmetry allows long measurement times. Our system ignores some properties of 3D polymeric systems including particle motion being restrained by an inert polymeric network, and entanglement of the polymeric binding sites.

A key criterion for our system to mimic the attachment of microscopic polymers is that the attachment positions of the magnetic heads and the resulting force fluctuations should be similar to those in macroscopic systems; that is the motion of the particles should be fairly random and the binding lifetimes exponentially distributed. In our system, up to six magnetic particles move because they are attached *via* a string to a speaker driven by Gaussian noise. In addition, we attached a weight to each string about halfway between the speaker attachment point and the particle. The additional weight reduced correlated motions between the magnetic particle and the speaker – just as two driven coupled pendula are chaotic. While several parameters in our system could be tuned, we focused on the amplitude of the speaker vibration and the number of strings, N. Varying the speaker amplitude changes the amount of energy provided to the systems which influenced both the binding kinetics and the properties of the yarn-weight system that are representative of changes in microscopic polymers. Varying the weights on the string will also have an effect on the width of the Gaussian distribution and the binding kinetics, an approach not taken in this paper.

Our devised system allows us to measure and tune the key parameters controlling the particle's motion due to binding of flexible polymers: the number of elastic tethers ($1 \leq N \leq 6$), their stiffness (measured as the width of the distribution of tether positions, σ by equivalence to Gaussian polymer chains with temperature T_c whose stiffness is given by $K = 2k_B T_c / 3\sigma^2$), the rate at which free tethers bind to the plate (k_a) and the rate
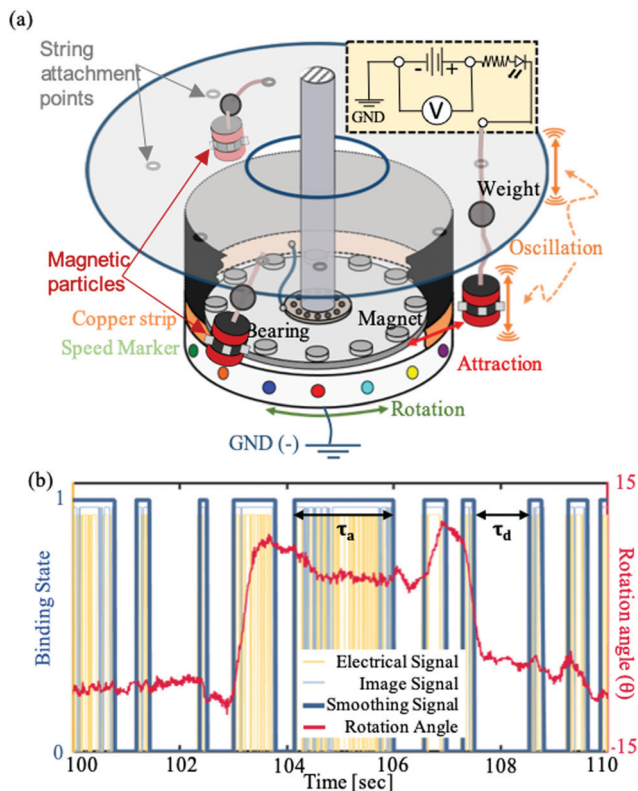
Fig. 2 (a) A macroscopic experimental model system designed to capture mechanical parameters for diffusion constant. The carousel plays the role of the plate, and the magnetic particles binding to the carousel act as the polymers. They are attached *via* strings ($1 \leq N \leq 6$), equally spaced around the carousel. (b) Life-time of attached state (τ_a) and detached state (τ_d) were obtained after smoothing the electrical or image raw data giving connectivity of tether (bound = 1 and free = 0) in time. The rotation angle θ was obtained from processing the image data.
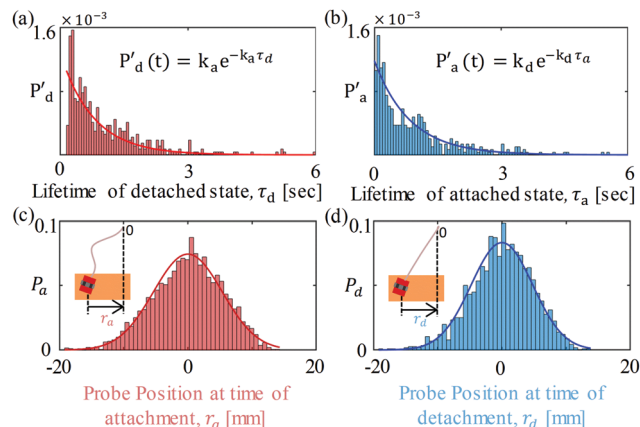

Fig. 3 (a) and (b) Probability histograms of the lifetimes of bound and free states of the tethers fitted with an exponential distribution of a Poisson process. (c) and (d) Statistical distribution of the position of the string, r_a and r_d during an attachment and detachment event fitted with a Gaussian distribution. These results are obtained with one tether ($N = 1$) and medium speaker power ($A = 17$ VAC).

at which bound tethers dissociate (k_d), (Fig. 2a). A camera recorded the position of both the center binding head and the cylinder. The attachment of the magnetic head to one of the cylinder's magnetic sites closed a circuit, providing an electrical readout of binding events. The two measurements were synchronized using images of LEDs in the electrical circuits. We found that the electrical signal was fairly noisy, but could easily be smoothed to give a reliable measurement of attachment. The noise during times when the magnetic particle was not bound appeared to be caused by unproductive collisions between the magnetic head and the copper strip. The motion of the magnetic head when bound also gave a noisy electrical signal (yellow lines in Fig. 2b). We smoothed the electrical signal by assuming that the shortest unbinding events were $\Delta t_{cr1} = 0.15$ s, and that the shortest binding events were $\Delta t_{cr2} = 0.015$ s. We confirmed that this smoothing resulted in an accurate representation of binding events by comparing the electrical signals with videos of the magnetic head's motion (Fig. 2b and Fig. S1b, ESI†).

From the measurement of both the binding state and the position of a head, we determined the distribution of lifetimes of the attached (τ_a) and detached (τ_d) states of the tethers

(Fig. 3a and b) and the position distribution of the head during attachment or detachments events (Fig. 3c and d). The binding distributions are well described by single exponential, and the position of attachment and detachment events follows a Gaussian distribution. We also note that increasing the number of chains do not significantly change the binding kinetics (see Table S1 of ESI†). Together, these demonstrate the applicability of this experimental system to the modeling of microscopic binding interactions.

We measured the effective diffusion constant D of the cylinder by tracking its angular position, θ, and calculating the mean squared angular displacement as a function of time t. We placed markers on the rotating cylinder and used Lagrangian tracking of markers near the center-line in high frame rate movies (120 FPS). The mean squared displacement (MSD) was computed as a temporal moving average $\langle \theta^2(t) \rangle = 1/(T - t) \int_0^{T-t} [\theta(t' - t) - \theta(t')]^2 dt'$, where $T \gg t$ is the total duration of the experiment.[28,29] The angular diffusion constant $D = (1/2) d\langle \theta^2 \rangle / dt$ was measured by running 18 different experiments for various combinations of N, and the speaker amplitude each for a duration of 15 min (data sets and videos are in the ESI†). Plotted are errors propagated from standard errors of the mean of the measured parameters, p, k_a, and k_d. There are additional systematic errors arising from the cylinder not being perfectly centered, variations in the tethers, and any residual forces from collisions between the magnetic head and cylinder that do not result in binding. Each data point corresponds to a different amplitude or number of strings. Together, these gave a good range of experimental parameters. In any diffusive process, the diffusion should increase with the size of steps, and decrease with the time between steps. As τ decreases, there will be more events each giving a small kick. On average, each kick will be larger as σ, the width of attachment positions, increases. In order to isolate the effects of binding affinity and number of strings, we scaled the diffusion constant by the typical length scale (σ_a), and the typical binding timescale $\tau = 1/(k_a + k_d)$, $D^\star = 2D/\sigma^2(k_a + k_d)$. What remains in the
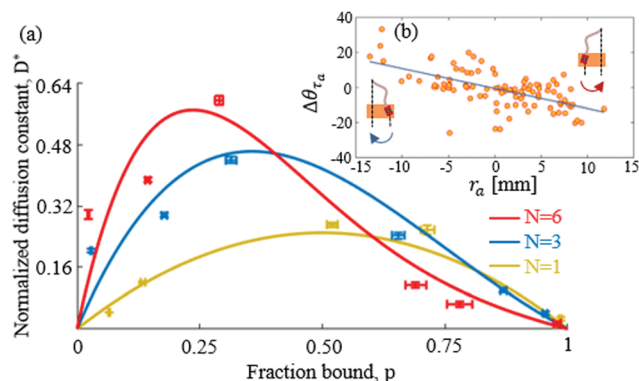
Fig. 4 (a) Plot of diffusion coefficient from experiments (error bars) analytical model (bold line) normalized as $D^* = 2D/\sigma^2(k_a + k_d)$ as a function of the ratio of rates $p = k_a/(k_a + k_d)$ with the different number of the binding site (or string head unit), $N = 1, 3, 6$. (b) Correlation between binding position r_a and the difference of angles during attachment event $\Delta\theta_{\tau a}$.

scaled diffusion constant are the dependencies on parameters specific to this system.

We found an optimum in the scaled diffusivity as we varied the fraction of time that each probe is bound, $p = k_a/(k_a + k_d)$ (Fig. 4). The maximum occurs at lower values of p as N increases. Holding the number of strings fixed, the measured diffusivity is the lowest and approaches zero in the extreme scenarios when hardly any tethers are bound ($p \to 0$), or all tethers are attached ($p \to 1$). In the first scenario, the plate receives no kicks from the tethers as none of them bind. As $p \to 1$ and $N > 1$ it is likely that there is already a string (or more) attached during binding events. The already-attached strings reduce the motion of the cylinder; the plate is trapped by being bound.

In contrast, in nearly all other diffuse processes governed by random kicks, D decreases monotonically with increasing particle size or viscosity. Here, the diffusion reaches its maximum value at particular combinations of number N of strings and binding and unbinding rates, k_a and k_d. The optimal size and binding kinetics are given by the dual nature of polymer attachments. On the one hand, binding events provide the driving force for particle motion. On the other hand, the higher number of bound particles, the higher the resistance to motion given by the previously attached strings. Our results may give insight into the observation of non-monotonic spreading of small molecules binders to a surface in the presence of competitors.[30]

Given this complex relationship, we sought to determine if we could understand the behavior of this system from a simple model of the particle motion. Our modeling efforts began with the observation that the distance traveled per binding event is correlated with the displacement of the magnet probe from center upon binding (Fig. 4 inset). This is exactly as expected for a microscopic polymeric system, where the polymer would act like an entropic string and provide a restoring force if it binds in its extended state (Fig. 1b). Our model, therefore, includes random binding of Hookean springs of spring constant, K, that once bound exert a force on the plate proportional to the spring

extension. We developed both analytical theory and Monte-Carlo simulations described in related theoretical work.[27] Good agreements are obtained between theory, experiment and simulation (Fig. 4a) for an extended range of microscopic parameters. This demonstrates the robustness of this behavior and the success of the prototypical design of a subunit to aid the building of an active metamaterial system.

In separating the diffusive motion due to chain binding and unbinding from that experienced by particles in microscopic systems due to the underlying fluid, we assumed that the system could be well described by a fluctuation–dissipation relation with an effective temperature. We sought to determine whether such a relationship could be experimentally tested by performing creep experiments to measure the resistive drag under an applied load. In order to apply a constant external torque, we wrapped the axle of our system with a string and attached the string *via* a pulley to a suspended weight (Fig. 5). We drove attachment and detachment events *via* the speaker as in the passive case (Fig. 5b). We predict that the angular creep velocity should be given by $\omega_{pre} = F/R\zeta_c = mgD_c/Rk_BT_c$ where m is the mass of the weight, g the acceleration due to gravity, and R the radius of the cylinder. For D_c we used our theoretical prediction based on the measured values for σ, k_a, and k_d, (Fig. 4). We independently calculated the effective temperature of a representative chain (the one chain visible in our movies) by $\frac{1}{2}m_c\langle v_{c,x}^2\rangle = \frac{1}{3}k_bT_c^{chain}$.

We performed a series of experiments varying the speaker amplitude and applied weight, all with $N = 3$ strings. We obtained a wide range of angular velocities, as shown in representative plots in Fig. 5b. Each trajectory was fit to a line with slope, ω_{obs}. As shown in Fig. 5b, there is a remarkably good agreement between the measured and predicted values of ω. A line of slope 1 is plotted as a guide to the eye, and is not a fit to the data. We conclude that, within the noise of our system, the drag and diffusivities are inversely proportional
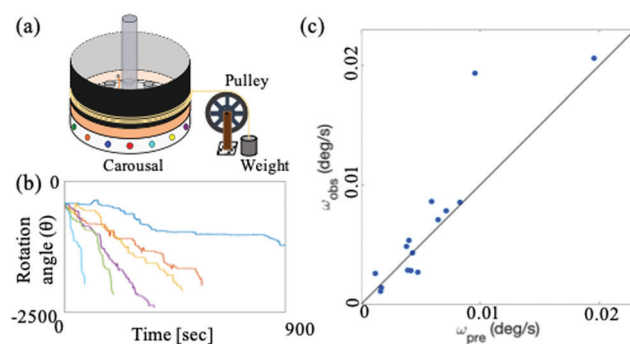

Fig. 5 (a) To measure the creep rate of the carousel under constant applied torque, we wrapped a string around the carousel, passed the string over a pully, and used it to suspend a weight. We drove attachment and detachment events as before. We used three different applied masses (m) and different speaker amplitudes to give a range of trajectories, a representative subset is shown in (b). (c) A plot of predicted ($\omega_{pre} = F/R\zeta_c = mgD_c/Rk_BT_c$) vs. measured ($\omega_{obs}$) average angular frequencies. A line of slope 1 is plotted as a guide to the eye.

with the proportionality constant given by the effective temperature measured assuming an equipartition relationship for the chains (approximately 8×10^{18} K for the drag experiments).

Taken together, this work demonstrates the feasibility of constructing a macroscopic analog to molecular systems whose structure and dynamics can be tuned for targeted applications. More specifically, our system was able to capture the complex relationship between the binding of flexible tethers and the resulting diffusive motion. Binding of flexible tethers drives particle motion, but the more tethers that are initially bound the stronger the restoring force resisting motion. The result is a diffusive behavior unlike most systems; here the diffusivity can be optimized for intermediate particle size (or in this case $\langle N_a \rangle$). However, this behavior is a key feature of diffusion through the nuclear pore complex and has common features with binding proteins of DNA.[13,31,32] While we have not explored correlations in binding events among tethers in this work, this work could serve as a starting point to better exploring such features. They become particularly highly relevant in multi-valent binding mechanisms in molecular systems like in the case of molecular spiders which involve multiple binding "legs" that can achieve random walk on receptor surfaces.[30,33] Because the experimental system could capture different regimes of binding-mediated diffusion, it maybe viewed as a proof-of-concept metamaterial whose structure/dynamics can be tuned to achieve programmable viscosity, particle segregation and transport. Extension of the proposed structure to two dimensions could mimic polymer brush structures with physical bonds,[34,35] or polymers with dynamic covalent chemistry.[36,37] Our work suggests that high multivalency but low affinity of each binding site could be ideal for rapid transport, a situation found in the nuclear pore complex.[38]

Conflicts of interest

There are no conflicts to declare.

Acknowledgements

References

1 P. Terech, V. Schaffhauser, P. Maldivi and J. M. Guenet, *Langmuir*, 1992, **8**, 2104–2106.

2 R. Marathe, C. Meel, N. C. Schmidt, L. Dewenter, R. Kurre, L. Greune, M. A. Schmidt, M. J. Müller, R. Lipowsky and B. Maier, *et al.*, *Nat. Commun.*, 2014, **5**, 1–10.

3 J. Witten, T. Samad and K. Ribbeck, *Curr. Opin. Biotechnol.*, 2018, **52**, 124–133.

4 F. J. Vernerey, R. Long and R. Brighenti, *J. Mech. Phys. Solids*, 2017, **107**, 1–20.

5 S. L. Sridhar and F. J. Vernerey, *J. Mech. Phys. Solids*, 2020, 104021.

6 T. Shen and F. J. Vernerey, *J. Mech. Phys. Solids*, 2020, 104028.

7 M. Kim, W. G. Chen, J. W. Kang, M. J. Glassman, K. Ribbeck and B. D. Olsen, *Adv. Mater.*, 2015, **27**, 4207–4212.

8 M. Kim, W. G. Chen, B. S. Souza and B. D. Olsen, *Mol. Syst. Des. Eng.*, 2017, **2**, 149–158.

9 Y. J. Yang, D. J. Mai, T. J. Dursch and B. D. Olsen, *Biomacromolecules*, 2018, **19**, 3905–3916.

10 J. Li, L. Fok, X. Yin, G. Bartal and X. Zhang, *Nat. Mater.*, 2009, **8**, 931–934.

11 S. Zhang, L. Yin and N. Fang, *Phys. Rev. Lett.*, 2009, **102**, 194301.

12 M. Doi, S. F. Edwards and S. F. Edwards, *The theory of polymer dynamics*, Oxford University Press, 1988, vol. 73.

13 T. Bickel and R. Bruinsma, *Biophys. J.*, 2002, **83**, 3079–3087.

14 A. Ghosh and K. S. Schweizer, *Macromolecules*, 2020, **53**, 4366–4380.

15 M.-H. Lu, L. Feng and Y.-F. Chen, *Mater. Today*, 2009, **12**, 34–42.

16 X. Ren, R. Das, P. Tran, T. D. Ngo and Y. M. Xie, *Smart Mater. Struct.*, 2018, **27**, 023001.

17 S. Banerjee, M. L. Gardel and U. S. Schwarz, *Annu. Rev. Condens. Matter Phys.*, 2020, **11**, 421–439.

18 C. P. Goodrich, M. P. Brenner and K. Ribbeck, *Nat. Commun.*, 2018, **9**, 4348.

19 Y. J. Yang, D. J. Mai, T. J. Dursch and B. D. Olsen, *Biomacromolecules*, 2018, 3905–3916.

20 L. Maguire, M. Stefferson, M. D. Betterton and L. E. Hough, *Phys. Rev. E*, 2019, **100**, 042414.

21 D. Osmanović, A. Fassati, I. J. Ford and B. W. Hoogenboom, *Soft Matter*, 2013, **9**, 10442–10451.

22 J. S. Mincer and S. M. Simon, *Proc. Natl. Acad. Sci. U. S. A.*, 2011, **108**, E351–E358.

23 L. Miao and K. Schulten, *Biophys. J.*, 2010, **98**, 1658–1667.

24 L. Maguire, M. D. Betterton and L. E. Hough, *Biophys. J.*, 2020, **118**(2), 376–385.

25 K. Ribbeck and D. Görlich, *EMBO J.*, 2001, **20**, 1320–1330.

26 B. Fogelson and J. Keener, *SIAM J. Appl. Math.*, 2019, 1405–1422.

27 S. Lalitha Sridhar, J. Dunnagin, K. Koo, L. Hough and F. Vernerey, 2021, DOI: 10.1021/acs.macromol.0c02306, to be published.

28 A. Lubelski, I. M. Sokolov and J. Klafter, *Phys. Rev. Lett.*, 2008, **100**, 250602.

29 A. Kusumi, Y. Sako and M. Yamamoto, *Biophys. J.*, 1993, **65**, 2021–2040.

30 A. Perl, A. Gomez-Casado, D. Thompson, H. H. Dam, P. Jonkheijm, D. N. Reinhoudt and J. Huskens, *Nat. Chem.*, 2011, **3**, 317–322.

31 B. Fogelson and J. P. Keener, *Biophys. J.*, 2018, **115**, 108–116.

32 P. Dey and A. Bhattacherjee, *Biophys. J.*, 2020, **118**, 505–517.

33 O. Semenov, M. J. Olah and D. Stefanovic, *Phys. Rev. E: Stat., Nonlinear, Soft Matter Phys.*, 2011, **83**, 021117.

34 T. F. A. de Greef and E. W. Meijer, *Nature*, 2008, **453**, 171–173.

35 M. J. Serpe and S. L. Craig, *Langmuir*, 2007, **23**, 1626–1634.

36 Y. Jin, Q. Wang, P. Taynton and W. Zhang, *Acc. Chem. Res.*, 2014, **47**, 1575–1586.

37 S. J. Rowan, S. J. Cantrill, G. R. L. Cousins, J. K. M. Sanders and J. F. Stoddart, *Angew. Chem., Int. Ed.*, 2002, **41**, 898–952.

38 R. Bayliss, T. Littlewood and M. Stewart, *Cell*, 2000, **102**, 99–108.